International Journal of Mass Spectrometry 281 (2009) 126–133

Contents lists available at ScienceDirect

International Journal of Mass Spectrometry

journal homepage: www.elsevier.com/locate/ijms

A combined database related and *de novo* MS-identification of yeast mannose-1-phosphate guanyltransferase PSA1 interaction partners at different phases of batch cultivation

Ville Parviainen[a], Sakari Joenväärä[a,b], Hannu Peltoniemi[a], Pirkko Mattila[b], Risto Renkonen[a,c,*]

[a] *Transplantation Laboratory and Infection Biology Research Program, Haartman Institute, Helsinki, Finland*
[b] *Medicel Ltd., Helsinki, Finland*
[c] *HUSLAB, Helsinki University Central Hospital, Helsinki, Finland*

ARTICLE INFO

Article history:
Received 12 December 2008
Received in revised form 9 January 2009
Accepted 13 January 2009
Available online 22 January 2009

Keywords:
Protein–protein interactions
Mass spectrometry
De novo protein identification

ABSTRACT

Mass spectrometry-based proteomic research has become one of the main methods in protein–protein interaction research. Several high throughput studies have established an interaction landscape of exponentially growing Baker's yeast culture. However, many of the protein–protein interactions are likely to change in different environmental conditions. In order to examine the dynamic nature of the protein interactions we isolated the protein complexes of mannose-1-phosphate guanyltransferase PSA1 from *Saccharomyces cerevisiae* at four different time points during batch cultivation. We used the tandem affinity purification (TAP)-method to purify the complexes and subjected the tryptic peptides to LC–MS/MS. The resulting peak lists were analyzed with two different methods: the database related protein identification program X!Tandem and the *de novo* sequencing program Lutefisk. We observed significant changes in the interactome of PSA1 during the batch cultivation and identified altogether 74 proteins interacting with PSA1 of which only six were found to interact during all time points. All the other proteins showed a more dynamic nature of binding activity. In this study we also demonstrate the benefit of using both database related and *de novo* methods in the protein interaction research to enhance both the quality and the quantity of observations.

1. Introduction

Protein interaction research is one of the cornerstone research areas in systems biology. Advances in methods and large scale protein–protein interaction experiments during the last 6 years have created a massive repository of interaction data for scientists to decipher [1–3]. The most common method of protein complex purification is the tandem affinity purification (TAP) method [4]. TAP-purification is followed by enzymatic digestion of the complexes and the resulting peptides are identified using mass spectrometry (MS) and bioinformatics [5,6]. Such experiments usually generate a vast amount of raw data and the major challenge is in how to link the information of the experimental conditions as well as *in silico* analysis methods to the actual interpreted data [7]. Without this crucial metadata the value of otherwise very expansive datasets is unfortunately limited.

Proteins are usually identified from raw mass spectrometry data with database related peptide identification in a high throughput manner [8]. While being quite efficient, accurate and allowing a wide range of user-specific modifications to original peptides it will miss unknown or unpredictably modified peptides [9]. An alternative approach is the *de novo* sequencing, where peptides are built from the tandem-MS data directly and all possible peptides of varying lengths within the parameters are listed [10]. These are further scored and finally matched against protein sequences using sequence alignment tools. The advantage of the *de novo* sequencing over database related identification is the tolerance against mutations and modifications [11]. The cost of *de novo* sequencing is the requirement for far more computer power than the database related searches.

To investigate the dynamic nature of protein complexes in yeast, we chose to isolate the interaction partners of the yeast mannose-1-phosphate guanyltransferase PSA1 (YDL055C) in various stages of its growth in batch culture. PSA1 is an essential yeast protein functioning in the mannose metabolism [12]. It converts mannose-1-phospate into GDP-mannose, which is utilized in the glycan biosynthesis, energy production and the cell wall metabolism (Fig. 1.).

* Corresponding author at: Transplantation laboratory & Infection Biology Research Program, Haartman Institute, University of Helsinki, PO Box 21, Haartman Institute (Haartmaninkatu 3), FIN-00014 Helsinki, Finland.
E-mail address: Risto.Renkonen@helsinki.fi (R. Renkonen).

1387-3806/$ – see front matter © 2009 Elsevier B.V. All rights reserved.
doi:10.1016/j.ijms.2009.01.005

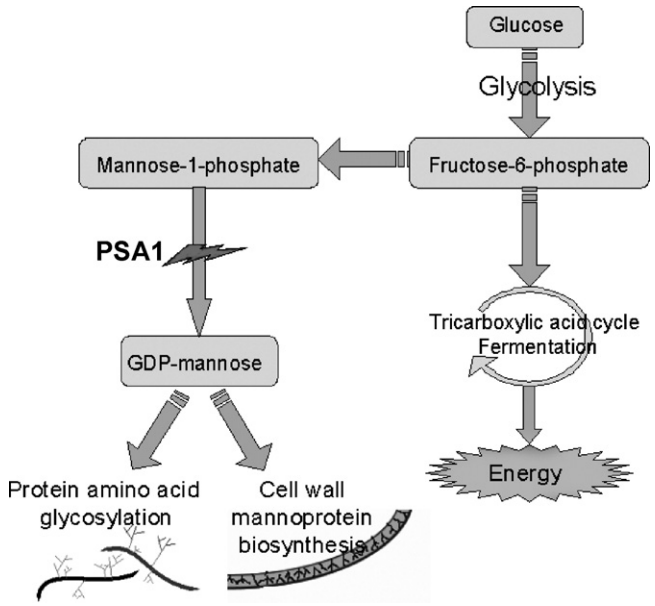

Fig. 1. The role of PSA1 in the energy/cell wall metabolism.

The isolated PSA1 binding partners were subjected to trypsin digestion and then to two-dimensional liquid chromatography coupled with mass spectrometry. The resulting MS-peak lists were analyzed with two different protein identification methods: the database related X!Tandem [13,14] and the *de novo* peptide sequencing program Lutefisk [15]. The Lutefisk *de novo* output was combined with modified NCBI BLAST sequence alignment tool for protein identification. The resulting protein lists were filtered based on the amount of peptides found for each protein. The protein identifications and the pre- and post-processing of the data were carried out using the Medicel Integrator software. The wet lab (i.e., experimental) and *in silico* metadata were attached to the protein identifications with variable description language (VDL) expressions and stored in the Medicel Integrator database. The VDL expressions consist of general keywords (such as time, species, compound, gene, protein, etc.) followed by values (exact time of sampling, exact subcellular location, name of the host strain, measured compound, gene identifier, protein identifier, etc.). VLD expressions are simply small textual tags attached to the measured or *in silico*-generated data. As they are fully computer-readable they can be used efficiently in filtering, querying and backtracking of the tagged data (www.medicel.com).

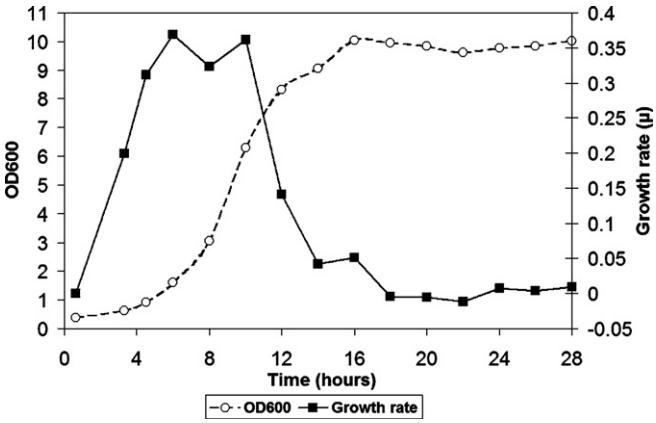

Fig. 2. The OD600 and growth rate during the batch cultivation.

Here we report major changes in the composition of PSA1 binding-proteins during batch cultivation at four time points (4, 8, 12 and 24 h after inoculum). The largest amount of interaction partners were found at the first two time points, when the cells were growing rapidly. At later time points, when the growth rate had decreased or even stopped, the PSA1 complex had markedly fewer members. Interesting changes were observed in interactions to ribosomal proteins as well as signaling, nuclear, cell wall and plasma membrane biosynthesis proteins. We also compared the efficiency of database related X!Tandem and *de novo* Lutefisk-BLAST-identification approaches. Our data illustrates that the use of these different methods in combination creates a more diverse set of proteins, but it also increases the confidence of the identification.

2. Experimental

2.1. Strain

PCR-based genomic tagging was used to fuse TAP-tag C-terminally to the PSA1 (YDL055C) gene according to the original method of Rigaut et al. [4]. The gene fusion cassette containing the TAP tag complements for the ura3 auxotrophy marker of the parental strain. The TAP fusion plasmid pBS1539 providing the TAP-tag next to the selectable marker as well as the host strain W303 (20000B;BMA64-1B) were purchased from Euroscarf (http://web.uni-frankfurt.de/fb15/mikro/euroscarf/).

2.2. Cultivation

The inocula for bioreactor cultivations were grown in eight 1000 ml Erlenmeyer shake flasks on 600 ml of YPD-medium. The inocula were started from 20 mg cell dry weight (CDW) of cells in glycerol stocks. The inocula were incubated at +30 °C for 16 h before inoculation to bioreactor. Bioreactor cultivation was performed in a 30-l Braun Biostat C-DCU instrument (B. Braun Biotech International GmbH, Meisungen, Germany) bioreactor. The cultivation temperature was +30 °C, agitation speed 800 rpm, initial cultivation volume 30 l, airflow 1.0 l/min, and pH 5.0 ± 0.2. The Verduyn (2X) mineral medium was used for the bioreactor cultivation.

2.3. Sampling

The samples for the protein complex identification were taken directly from the bioreactor. Samples were taken at four time points: 4 h, 8 h, 12 h and 24 h from the inoculum. The OD600 and growth rate curve are represented in Fig. 2 The OD600 values were 0.92 for 4 h, 3.05 for 8 h, 8.33 for 12 h and 9.77 for 24 h samples. The growth rates were $\mu(4\,h) = 0.31$, $\mu(8\,h) = 0.32$, $\mu(12\,h) = 0.14$ and $\mu(24\,h) = 0.008$.

All sample volumes were 5 l. After sampling the yeast cells were pelleted by centrifugation 12 900 × *g* at +4 °C for 5 min. There appeared a dip in the growth rate curve at time point two (8 h) indicating protracted growth. However, the growth rate measurements taken at 6 and 10 h after inoculation are both ~0.36 suggesting that the rate of growth is constant and that the dip is due to an error in OD measurement.

2.4. TAP-isolation

The tandem affinity purification was done basically as described by Rigaut et al. (http://www-db.embl-heidelberg.de/jss/servlet/de.embl.bk.wwwTools.GroupLeftEMBL/ExternalInfo/seraphin/TAP.html) [4]. All used solutions were at +4 °C and samples were kept on ice or at +4 °C. The yeast cells were lysed with a Bead-Beater apparatus (Bead Beater, Model 1107900, Biospec Products Inc, Bartesville, OK) with 0.5 mm diameter glass beads (Biospec

Products Inc.). A lysis chamber (volume 350 ml) was filled with 200 ml of cold glass beads and the cell suspension was added. The chamber was filled to the top with NP-40 buffer [6 mM Na_2HPO_4, 4 mM NaH_2PO_4, 1% Igepal CA-630 (NP-40), 150 mM NaCl, 2 mM EDTA, 50 mM NaF, 0.1 mM Na_3VO_4] with protease inhibitors PMSF (1 mM) and EDTA Free Protease Inhibitor Cocktail Tablets (Roche Diagnostics GmbH, Mannheim, Germany) and immersed in an ice-water jacket. Lysis was performed with twelve 20 s bursts with a 40-s cooling period. The cell lysis was verified with microscope. The lysate was pre-cleared by centrifugation of 3200 × *g* at +4 °C for 5 min. The supernatant was further cleared by centrifugation of 99 000 × *g*, +4 °C for 30 min. The visible lipid layer was carefully removed. The supernatant was collected in 50 ml Falcon tubes and 200 μl of IgG sepharose beads was added to each tube. The IgG incubation was performed with gentle rotation at +4 °C for 2 h. The beads were allowed to sediment for 20 min and then transferred to a column. The beads were washed three times with 10 ml of IPP150 buffer (10 mM Tris–HCl pH 8.0, 150 mM NaCl, 0.1% NP-40) and once with 10 ml of TEV cleavage buffer (10 mM Tris–HCl, pH 8.0, 150 mM NaCl, 0.1% NP-40, 0.5 mM EDTA, 1.0 mM dithiothreitol added just before use). The beads were suspended to 2 ml of TEV cleavage buffer and transferred to 15 ml Falcon tubes. 450 units of TEV protease was added and then incubated overnight at +16 °C with gentle rotation. The suspension was then transferred to column and the eluate was collected. The IgG beads in column were rinsed once with 1 ml of TEV cleavage buffer, which was collected to same tube as the eluate. Three volumes (~7 ml) of calmodulin binding buffer (10 mM Tris–HCl, pH 8.0, 150 mM NaCl 1 mM Mg^{2+}-acetate, 1 mM imidazole, 2 mM $CaCl_2$, 10 mM-mercaptoethanol added just before use) 7 μl of 1 M $CaCl_2$ and 300 μl of calmodulin beads were added to the eluate. This was incubated at +4 °C for 1 h with gentle rotation. The suspension was then transferred to a column and first washed twice with 10 ml of calmodulin binding buffer with 0.1% NP-40 and then once with 10 ml of calmodulin binding buffer with 0.02% NP-40. The proteins were eluted with 1.5 ml of calmodulin elution buffer (10 mM Tris–HCl pH 8.0, 150 mM NaCl, 0.02% NP-40, 1 mM Mg^{2+} -acetate, 1 mM imidatzole, 20 mM EGTA, 10 mM-mercaptoethanol added just before use).

2.5. TCA precipitation

The purified complexes were precipitated with solid trichloroacetic acid to final concentration of 25% (w/v) and incubated on ice for 30 min with periodic vortexing. The precipitated proteins were pelleted by centrifugation at +4 °C for 30 min of at 16 100 × *g*. The pellet was washed once with 0.05 N HCl in ice-cold acetone, centrifuged at 16 100 × *g* for 5 min at +4 °C and then washed with ice-cold acetone and centrifuged as previously. The pellet was finally dried in Savant Speed Vac concentrator (Savant Instruments, Farmingdale, NY).

2.6. Mass spectrometry sample preparation

The protein pellet was suspended in 50 mM $NaHCO_3$ (pH 8.5) and trypsin (Sequencing Grade Modified Trypsin, Promega, Madison WI) was added to a final concentration of 12.5 ng/μl. The proteins were digested at +37 °C overnight and stored −70 °C until used.

2.7. Mass spectrometry

The mass spectrometry was performed using a Waters Micromass nanoLC CapLC coupled to QTOF Ultima Global mass spectrometer. In the nanoLC CapLC system, a reversed-phase trapping column Waters Symmetry300, C18, 5 μm, 300 Å, i.d. 0.18 mm × 23 mm was used and as an analytical column a LC Packings PepMap100, C18, 5 μm, 100 Å, 75 μm i.d. × 25 cm. Mobile phase A: 0.1% formic acid in 5% MeCN and B: 0.1% formic acid in 95% MeCN. The sample was acquired for 600 min in the positive ion mode using the variable flow technique with gradient from 95% A to 5% A. Flow rate was 300–400 nl/min. Mass spectrometry acquisition details are available in the supplement. The peak list was calculated from the raw data using Mascot Distiller software (version 2.1.1.0, Matrix Science, London, UK) and saved as .mgf format.

2.8. In silico methods analysis workflow

The automated workflow for peptide identification and analysis is hierarchical and contains several subworkflows (Fig. 3.). The dark-grey boxes represent subworkflows, the light-grey boxes output files (results) from them and concomitantly input files for the next subworkflows.

The first subworkflow retrieves the FASTA amino acid sequences from Swissprot database (version 53.2; 23.10.2007) for all yeast *Saccharomyces cerevisiae* proteins (a) and outputs them in VDL-format. This is used in the subsequent subworkflow, which calculates the peptide and protein scores for all four time points using the database related X!Tandem and *de novo* MS/MS interpretation program Lutefisk (b.). X!Tandem searches were conducted using two parameter settings: trypsin with no more than two misscleavages and with no enzyme specificity and maximum of 50 missed cleavages. The X!Tandem (version X!TANDEM 2; 2007.07.01.2; http://www.thegpm.org/TANDEM/) parameters for trypsin limited search were: spectrum parameters ±0.2 Da for the parent monoisotopic mass error and ±0.1 Da for the fragment monoisotopic mass error; for the spectrum conditioning a dynamic range of 100 was used with total spectrum peaks of 50, maximum parent charge 4, minimum parent M+H of 500.0 and minimum fragment *m*/*z* 150.0; oxidation of methionine, acetylation of N-terminus, deamination of asparigine and glutamine were specified as potential residue modifications. As our goal was to identify as much proteins as possible from low to high abundance proteins, the QTOF parameters were adjusted in this case towards the sensitivity at the cost of resolution. As the theoretical amount of tryptic peptides in the yeast proteome is rather small (compared for human proteome for example) and the QTOF tuned for high sensitivity (low resolution), the larger search window is needed than when operating QTOF in the highest possible resolution. Even thought the used search windows are rather wide, most of our typical peptide delta masses for identified peptides fell well below 0.1 Da.

Enzyme was set to trypsin with the maximum of two missed cleavages. The other X!Tandem identification was performed with the same parameters except no enzyme was selected for cleavage and the maximum of missed cleavages was set to 50. Amino acid sequences for the protein identification and the sequence alignment were from SwissProt. For Lutefisk (version LutefiskXP v1.0.4; http://www.hairyfatguy.com/lutefisk/) the spectrum parameters were ±0.4 Da for the parent monoisotopic mass error and 0.2 Da for the fragment monoisotopic mass error. Potential residue modifications for Lutefisk were the same as for X!Tandem searches. The alignment of the *de novo* peptides to protein sequences from SwissProt was performed with Blastall program (version 2.2.14, May-07-2006 from NCBI; http://www.ncbi.nlm.nih.gov/). The parameters for Blastall were: wordsize 2; expectation value 0.1; threshold for extending hits 11 and no gapped alignment. Complete X!Tandem and Lutefisk parameters are represented in Supplementary file S1.

The results from all three methods (X!Tandem-trypsin limited, X!Tandem-no enzyme and Lutefisk-BLAST) (c) and all time points are annotated in the next subworkflow by attaching the time point and the method of detection with VDL-expressions. The results are finally combined to one single dataset containing the identified pro-

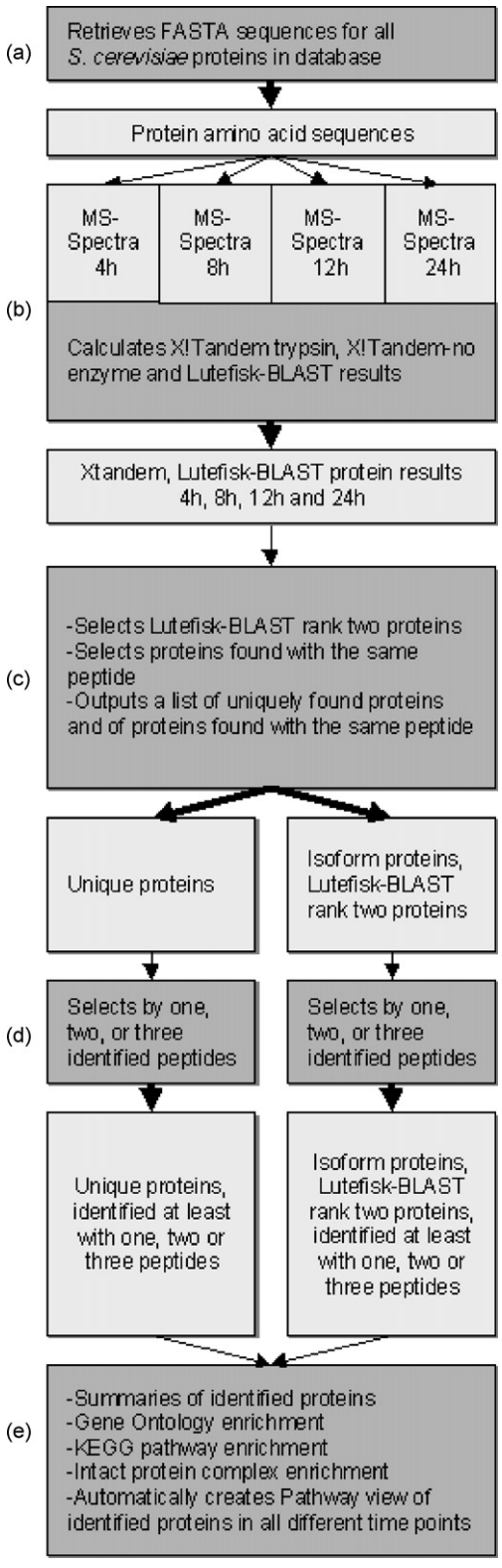

Fig. 3. The workflow flow chart. The dark grey background indicates a subworkflow and light grey background a result data set of each subworkflow.

teins, the time point of the detection, and the method of detection. The variables for each protein are: X!Tandem group, mudpit-score, protein-score, X!Tandem rank, the coverage of protein amino acid sequence, the number of peptides, the number of unique peptides, the number of unique spectra for each protein and the number of unique spectra of unique peptides. All results for both peptide and protein identifications are represented in Supplementary files S2 and S3.

The X!Tandem and Lutefisk-BLAST outputs contain some proteins, mainly ribosomal isoforms, where the identified peptide used in identification matches two or more proteins. Such proteins are automatically combined in a separate isoform list along with Lutefisk-BLAST rank-two proteins. This list is processed identically with the list of unique protein hits.

The following subworkflow (d) filters the results by the user specified protein variable such as the score or the amount of peptides used in the identification. In this study we used one, two, or three peptides as cut-off limits. The last subworkflow is used in automatic analysis of the resulting data sets. The workflow creates a summary of the amounts of proteins identified with different methods and the commonalities between the methods. The filtered list of proteins with their respective variables is also displayed. The same workflow enriches the protein data sets to Gene Ontology [16], KEGG pathways [17] and to Intact protein complexes [18]. As a quality control, the found interaction partners are compared to known PSA1 interaction partners from SGD (saccharomyces genome database) [19]. Finally the subworkflow annotates and stores the new connections to the Medicel Integrator database. The subworkflow simultaneously creates an interaction view of all the elements such as compounds, genes and protein complexes and the connections between the prey proteins and these elements. The connections are all retrieved from the Integrator database and can be viewed with the Integrator Pathway application.

3. Results and discussion

Our purpose was to elucidate the changing interactome of PSA1 during batch cultivation and to automate the analysis by using software to attach experimental and *in silico* metadata with interpretations. We chose the time points of sampling to represent the different phases of growth in cell culture. At 4 h the culture has just passed the initial lag phase and the cell culture is adapting to fast growth. 8 h represents the time of logarithmic growth, at 12 h the cellular density has greatly expanded and the lack of nutrients is already limiting growth. At 24 h the yeast cell culture has adapted to starvation and adjusted the internal state to very slow growth.

3.1. The effect of the analysis method and peptide limit to identification

To allow a meaningful comparison of the number of identified proteins, each identified peptide from the MS/MS analysis was allowed to yield only one protein interpretation, i.e., the duplicate protein hits from the isoform list were deleted. When the identification was based on only one peptide, 235 distinct proteins interacting with PSA1 were found. All methods were equally efficient as X!Tandem-trypsin identified 106, X!Tandem-no enzyme 108 and Lutefisk-BLAST found 112 different proteins. While 31 proteins were found with all methods X!Tandem-trypsin recognized 46, X!Tandem-no enzyme 48 and Lutefisk-BLAST 81 unique proteins.

More stringent analysis showed that out of the 112 proteins identified by Lutefisk-BLAST with one peptide, 24 passed the two-peptide limit and only seven were identified with three peptides or more, while X!Tandem-no enzyme yielded 35 and 29 distinct proteins respectively. The best results were obtained with X!Tandem-trypsin limited search. From the original 106 proteins identified with one peptide, 58 were observed with two and 38 with three or more peptides. The overall number of distinct proteins decreased from 236 to 74 with the two-peptide- and to 43 with the three-peptide limit.

Table 1
Identified proteins at different time points.

Medicel Integrator-Swissprot name	SGD name	Description	4 h	8 h	12 h	24 h
Non-ribosomal proteins						
MP_MPG1_YEAST	PSA1	Mannose-1-phosphate guanyltransferase	2	2	2	2
MP_MANA_YEAST/026375768	PMI40	Mannose-6-phosphate isomerase	2	ND	ND	2
MP_ESR1_YEAST	MEC1	Serine/threonine-protein kinase MEC1	2	2	2	ND
MP_YNR6_YEAST	YNL176C	Uncharacterized protein YNL176C	2	2	2	2
MP_IMD3_YEAST	IMD3	Probable inosine-5'-monophosphate dehydrogenase IMD3	2	ND	ND	ND
MP_HS60_YEAST	HSP60	Heat shock protein 60\, mitochondrial precursor	ND	2	ND	ND
MP_SC16_YEAST	SEC16	Multidomain vesicle coat protein	ND	2	ND	ND
MP_DPOG_YEAST	MIP1	DNA polymerase gamma	ND	2	ND	ND
MP_N145_YEAST	NUP145	Nucleoporin NUP145 precursor	ND	2	ND	ND
MP_CK11_YEAST	YCK1	Casein kinase I homolog 1	ND	2	ND	ND
MP_Q07653	HBT1	Protein HBT1	1	2	2	1
MP_Q06674	HIM1	Protein HIM1	ND	2	ND	ND
MP_Q08951	APL5	AP-3 complex subunit delta	ND	ND	2	ND
MP_Q12139	YPR022C	Zinc finger protein YPR022C	1	ND	2	2
MP_VATB_YEAST	VMA2	Vacuolar ATP synthase subunit B	ND	ND	ND	2
MP_KPY1_YEAST	CDC19	Pyruvate kinase 1	ND	ND	ND	2
MP_YIJ2_YEAST	YIL092W	Uncharacterized protein YIL092W	1	ND	1	2
MP_UFD4_YEAST	UFD4	Ubiquitin fusion degradation protein 4	ND	ND	ND	2
MP_Q08930	YPL191C	Uncharacterized protein YPL191C	ND	1	ND	2
MP_METK_YEAST	*SAM1*	*S-adenosylmethionine synthetase 1*	*2*	*2*	*ND*	*2*
MP_METL_YEAST/026373382	*SAM2*	*S-adenosylmethionine synthetase 2*	*2*	*2*	*ND*	*2*
MP_ORC2_YEAST	***ORC2***	***Origin recognition complex subunit 2***	***2***	***2***	***1***	***2***
MP_YML8_YEAST	***NGL3***	***Probable RNA exonuclease NGL3***	***ND***	***2***	***1***	***ND***
MP_GAL4_YEAST	***GAL4***	***Regulatory protein GAL4***	***ND***	***2***	***2***	***1***
MP_HMD1_YEAST	***HMG1***	***3-hydroxy-3-methylglutaryl-coenzyme A reductase 1***	***ND***	***2***	***1***	***ND***
MP_HMD2_YEAST	***HMG2***	***3-hydroxy-3-methylglutaryl-coenzyme A reductase 2***	***ND***	***2***	***1***	***ND***
MP_SA155_YEAST	***SAP155***	***SIT4-associating protein SAP155***	***ND***	***2***	***ND***	***ND***
MP_ARO1_YEAST	***ARO1***	***Pentafunctional AROM polypeptide***	***ND***	***2***	***ND***	***2***
MP_YKM1_YEAST	***YKL121W***	***WD repeat protein YKL121W***	***1***	***2***	***ND***	***ND***
MP_Q06412	***TUS1***	***Rho1 guanine nucleotide exchange factor TUS1***	***ND***	***1***	***ND***	***2***

Medicel Integrator-Swissprot name	SGD name	Description	Time1	Time2	Time3	Time4
Ribosomal proteins						
MP_RS3_YEAST/026362256	RPS3	40S ribosomal protein S3	2	2	ND	1
MP_RL25_YEAST/026353826	RPL25	60S ribosomal protein L25	2	2	2	1
MP_RL10_YEAST	RPL10	60S ribosomal protein L10	2	2	ND	1
MP_RS7A_YEAST/026358212	RPS7A	40S ribosomal protein S7-A	2	2	ND	ND
MP_RS3A_YEAST/026363581	RPS1A	40S ribosomal protein S1-A	2	ND	1	ND
MP_RS2_YEAST/026363485	RPS2	40S ribosomal protein S2	2	2	ND	ND
MP_RS15_YEAST	RPS15	40S ribosomal protein S15	2	ND	ND	ND
MP_RS3B_YEAST/026363577	RPS1B	40S ribosomal protein S1-B	2	ND	ND	ND
MP_RL7A_YEAST/026362576	RPL7A	60S ribosomal protein L7-A	2	ND	ND	ND
MP_RL17A_YEAST	RPL17A	60S ribosomal protein L17-A	2	2	ND	ND
MP_RL33A_YEAST	RPL33A	60S ribosomal protein L33-A	2	ND	ND	ND
MP_RL2_YEAST/026363477	RPL2BRPL2A	60S ribosomal protein L2	2	2	1	2
MP_RS8_YEAST/026359159	RPS8A RPS8B	40S ribosomal protein S8	2	2	1	2
MP_RS6_YEAST	RPS6A RPS6B	40S ribosomal protein S6	2	2	1	ND
MP_RS18_YEAST/026205974	RPS18A RPS18B	40S ribosomal protein S18	2	2	ND	ND
MP_RS16_YEAST/026353995	RPS16A RPS16B	40S ribosomal protein S16	2	2	ND	ND
MP_RS11_YEAST/026355517	RPS11A RPS11B	40S ribosomal protein S11	2	1	ND	ND
MP_RS4_YEAST/026364212	RPS4A RPS4B	40S ribosomal protein S4	2	ND	ND	2
MP_RS24_YEAST/026352943	RPS24A RPS24B	40S ribosomal protein S24	2	ND	ND	1
MP_RL16B_YEAST	RPL16B	60S ribosomal protein L16-B	1	2	ND	ND
MP_RL3_YEAST/026373502	RPL3	60S ribosomal protein L3	ND	2	ND	ND
MP_R13A_YEAST	RPL13A	60S ribosomal protein L13-A	ND	2	1	ND
MP_RL6A_YEAST/026357068	RPL6A	60S ribosomal protein L6-A	ND	2	1	ND
MP_RL20_YEAST/026356771	RPL20B RPL20A	60S ribosomal protein L20	ND	2	ND	ND
MP_RL19_YEAST/026358147	RPL19B RPL19A	60S ribosomal protein L19	1	2	ND	ND
MP_RS23_YEAST	RPS23A RPS23B	40S ribosomal protein S23	ND	2	2	ND
MP_RL18_YEAST	RPL18A RPL18B	60S ribosomal protein L18	ND	2	2	ND
MP_RL32_YEAST	RPL32	60S ribosomal protein L32	ND	1	ND	2
MP_RL26A_YEAST	RPL26A	60S ribosomal protein L26-A	ND	ND	*2*	*1*
MP_RL23_YEAST/026198035	RPL23A RPL23B	60S ribosomal protein L23	ND	ND	*2*	*1*
MP_RL4B_YEAST/026371953	*RPL4B*	*60S ribosomal protein L4-B*	*2*	*2*	*ND*	*2*
MP_RL4A_YEAST/026371952	*RPL4A*	*60S ribosomal protein L4-A*	*2*	*2*	*ND*	*2*
MP_R13A_YEAST	*RPL13A*	*60S ribosomal protein L13-A*	*2*	*ND*	*ND*	*ND*
MP_R13B_YEAST	*RPL13B*	*60S ribosomal protein L13-B*	*2*	*2*	*ND*	*2*
MP_RL7B_YEAST/026362593	*RPL7B*	*60S ribosomal protein L7-B*	*2*	*2*	*ND*	*2*
MP_RL31A_YEAST	*RPL31A*	*60S ribosomal protein L31-A*	*2*	*ND*	*1*	*ND*
MP_RL31B_YEAST	*RPL31B*	*60S ribosomal protein L31-B*	*2*	*ND*	*ND*	*1*
MP_RL17B_YEAST	*RPL17B*	*60S ribosomal protein L17-B*	*2*	*2*	*ND*	*1*
MP_RL27B_YEAST	*RPL27B*	*60S ribosomal protein L27-B*	*2*	*2*	*1*	*ND*
MP_RL27A_YEAST	*RPL27A*	*60S ribosomal protein L27-A*	*2*	*2*	*1*	*ND*
MP_RS22B_YEAST/026352350	*RPS22B*	*40S ribosomal protein S22-B*	*2*	*ND*	*ND*	*ND*

Table 1 (*Continued*)

Medicel Integrator-Swissprot name	SGD name	Description	Time1	Time2	Time3	Time4
MP_RS22A_YEAST/026352349	*RPS22A*	*40S ribosomal protein S22-A*	*2*	*ND*	*ND*	*ND*
MP_RL36B_YEAST	*RPL36B*	*60S ribosomal protein L36-B*	*2*	*1*	*1*	*ND*
MP_RL36A_YEAST	*RPL36A*	*60S ribosomal protein L36-A*	*2*	*1*	*1*	*ND*
MP_RL11B_YEAST/026356891	*RPL11B*	*60S ribosomal protein L11-B*	*2*	*ND*	*ND*	*ND*
MP_RL11A_YEAST/026356900	*RPL11A*	*60S ribosomal protein L11-A*	*2*	*ND*	*ND*	*ND*
MP_RL15B_YEAST	*RPL15B*	*60S ribosomal protein L15-B*	*2*	*1*	*1*	*ND*
MP_RL15A_YEAST	*RPL15A*	*60S ribosomal protein L15-A*	*2*	*1*	*1*	*ND*
MP_RL17A_YEAST	*RPL17A*	*60S ribosomal protein L17-A*	*2*	*2*	*1*	*ND*
MP_R17A_YEAST	*RPS17A*	*40S ribosomal protein S17-A*	*ND*	*2*	*1*	*2*
MP_R17B_YEAST	*RPS17B*	*40S ribosomal protein S17-B*	*ND*	*2*	*1*	*2*
MP_RS14B_YEAST	*RPS14B*	*40S ribosomal protein S14-B*	*ND*	*2*	*ND*	*ND*
MP_RS14A_YEAST	*RPS14A*	*40S ribosomal protein S14-A*	*ND*	*2*	*ND*	*ND*
MP_R14B_YEAST	*RPL14B*	*60S ribosomal protein L14-B*	*ND*	*2*	*ND*	*ND*
MP_R14A_YEAST	*RPL14A*	*60S ribosomal protein L14-A*	*ND*	*2*	*2*	*ND*
MP_RL26A_YEAST	*RPL26A*	*60S ribosomal protein L26-A*	*1*	*2*	*ND*	*ND*
MP_RL26B_YEAST	*RPL26B*	*60S ribosomal protein L26-B*	*1*	*2*	*ND*	*ND*
MP_RL7A_YEAST/026362576	*RPL7A*	*60S ribosomal protein L7-A*	*ND*	*2*	*ND*	*ND*
MP_RL8B_YEAST/026363653	*RPL8B*	*60S ribosomal protein L8-B*	*1*	*2*	*ND*	*1*
MP_RL8A_YEAST/026363650	*RPL8A*	*60S ribosomal protein L8-A*	*1*	*2*	*ND*	*1*
MP_RL33B_YEAST	*RPL33B*	*60S ribosomal protein L33-B*	*1*	*2*	*ND*	*1*
MP_RL33A_YEAST	*RPL33A*	*60S ribosomal protein L33-A*	*1*	*2*	*ND*	*1*

The proteins identified with the same peptide (isoforms) are in italics and the Lutefisk-BLAST rank-two proteins in italics and bold. ND = not detected, 1 = identified with only one peptide at the time point, 2 = identified with at least two-peptides at the time point.

To assess the accuracy of our identification, the combined list of proteins over all time points was compared to known affinity purified PSA1 complex members from SGD. Of the reference set of 74 individual PSA1 interaction partners (10.4.2008) we were able to identify 18 proteins, when the peptide limit was set to one. Of these 16 were identified with X!Tandem-trypsin, 15 with X!Tandem-no enzyme and 11 with Lutefisk-BLAST and 9 were common to all methods.

In a more stringent analysis, X!Tandem-trypsin identified the highest number of SGD reference proteins, i.e., 13 in two-peptide and 10 in three-peptide limit. Results with X!Tandem-no enzyme decreased from 15 to nine proteins with at least two-peptides and to seven with three peptides or more. The reduction in the amount of proteins identified by Lutefisk-BLAST was more pronounced as we could identyfy eleven SGD proteins with at least one peptide, six of those remained in the two-peptide limit and two proteins in the three peptides or more set.

Judged by the amount of identified proteins and the coverage of SGD reference proteins, the X!Tandem with trypsin limited parameters performed the best. With peptide limit set to one or more, all methods identified almost the same number of proteins. When the peptide limit was raised to two and three, the number of X!Tandem-no enzyme and especially Lutefisk-BLAST identified proteins declined considerably. However the combined use of database related X!Tandem and *de novo* identification program Lutefisk is advantageous, especially in the one peptide or more limited set. Assigning a cut off of more than one peptide will produce a more reliable set of stable and high-affinity interactions, but it may miss completely the transient and low-abundance complex partners. Such temporary interactions are important in the many signaling events and regulation of numerous biological processes. Thus simultaneous use of database related and the *de novo* protein identification method creates a richer set of possible complex members. It also produces an additional layer of confidence especially with those proteins found to be common with both methods. The benefit of Lutefisk is also evident in cases where the large amount of prey peptides masks the peptides derived from the possibly low abundance interaction partners. Such is the case with known PSA1 interaction partners SAP155 and ARO1. ARO1 is found in the 8-h sample and SAP155 in the 8- and 24-h samples by Lutefisk-BLAST only and as rank-two proteins. The rank-one protein in both instances is the bait PSA1. The benefit of using X!Tandem with no enzyme specificity is not as evident. It does provide additional unique identifications in one peptide set yet it roughly produces the same results as X!Tandem-trypsin, but with lower coverage. In addition it is computationally very heavy in cases where there is a large amount of MS spectra to decipher.

3.2. The change in interactions to ribosomal proteins in different time points

For examination of the proteins found at each time point, we included the isoforms and Lutefisk-BLAST rank-two proteins. We also included those proteins that pass the two-peptide limit in one time point, but are also found in other time points with only one peptide. All identified proteins are represented in Table 1. In this research we observed major changes in the interactome of PSA1 depending on the sampling time. Most notable changes were seen in the Gene Ontology category Ribosome. At the first time point of 4 h after inoculum we were able to identify 46 ribosomal proteins (21 with unique peptides and 25 in isoform list). At the second-time point of 8 h, the number of ribosomal proteins was again 46 (21 unique, 25 isoform). At time point three the number of ribosomal interactions fell to just 22 proteins (11 unique and 11 isoform, most proteins with only one peptide), and 22 proteins (10 unique, 12 isoform) at time point four.

This notable change in PSA1 interactions with the protein biosynthesis machinery may be attributed to the changes in the speed of translation and the requirement of PSA1 in rapidly growing yeast cells at the first two time points. As cells divide rapidly in excess amounts of glucose and nutrients, the overall protein synthesis rate is high. This could reflect the abundance of ribosomal proteins found interacting with PSA1 at the first two time points. As the availability of glucose and other nutrients becomes scarce at the last two time points, the requirement for cell wall biosynthesis proteins also decreases. This may lead to the reduction of ribosomes producing PSA1 thus affecting the identification of interacting ribosomal proteins at these time points. Another explanation for the changes in ribosomal interactions could be that the interactions are mainly artifacts and reflect only the relative abundance of ribosomal proteins at each time point.

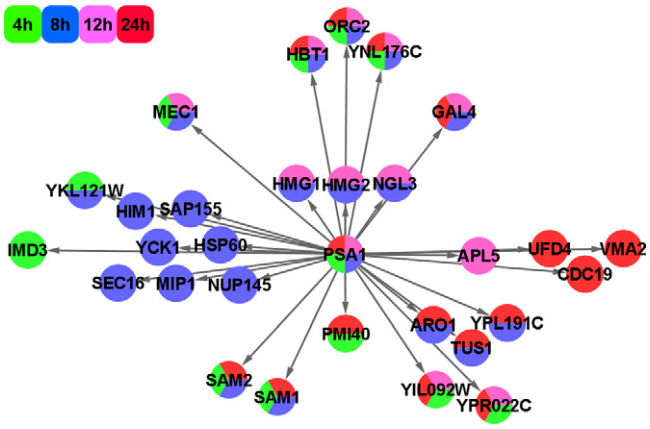

Fig. 4. The network of the PSA1 non-ribosomal interactions. The proteins are organized by detection time from left to right and color-coded based on the detection time point. The protein names are given in Swissprot format.

3.3. Changes in interactions to non-ribosomal proteins

Similar changes were observed with non-ribosomal proteins also especially at the second-time point. Of the 29 non-ribosomal proteins identified in the two or more-peptide limited set, 21 were observed at the second-time point. The network of all interactions at different time points is represented in Fig. 4.

As the identification of most proteins varied at different time points throughout the cultivation, three were found at all four sampling points. The three common proteins were YNL176C—an uncharacterized cell-cycle regulated protein [20], HBT1—a widely phosphorylated protein participating in bud site selection and cell morphogenesis [21] and ORC2 (found with Lutefisk-BLAST as rank-two protein), a subunit of the origin of the recognition complex [22,23].

Judged by our results, the interactome of PSA1 is quite complex. We can find interactions with proteins in different subcellular locations as well as in different functional categories. PSA1 has interactions with enzymes that participate in pathways producing essential plasma membrane sterols and phospholipids but also in GTP producing, energy and amino acid pathways. In the energy producing pathways PSA1 interactions include PMI40 and CDC19. CDC19 is a key enzyme in glycolysis as it catalyzes the conversion of phosphoenolpyruvate into pyruvate, an important branch point in the energy as well as in many other biosynthesis pathways [24,25]. Likewise PMI40 converts the glycolytic intermediate fructose-6-phosphate into mannose-6-phosphate thus linking the energy metabolism to the biosynthesis of cell wall proteins [26]. ARO1 catalyzes several steps in chorismate biosynthesis pathway with erythrose-4-phosphate leading to aromatic amino acids and folate [27]. Erythrose-4-phosphate can additionally be used with xylulose-5-phosphate in non-oxidative branch of pentose phosphate pathway to produce fructose-6-phosphate (a substrate for PMI40) and glyceraldehyde-3-phosphate, both intermediates of glycolysis. Additionally, the first and the second to last steps in chorismate biosynthesis use phosphoenolpyruvate as substrates, linking ARO1 again to glycolysis and energy metabolism. The PSA1 interaction partners involved in plasma membrane biosynthesis pathways are differentially regulated SAM1 or SAM2 (isoforms, identified with identical peptide) that produce *S*-adenosylmethionine [28–30] and HMG1 or HMG2 of the sterol biosynthesis pathway [31]. *S*-adenosylmethionine is an important methyl donor in a wide number of reactions such as the biosynthesis of phospholipids and production of ergosterol, another major plasma membrane molecule. A key intermediate in the ergosterol biosynthesis is mevalonate produced by rate-liming enzymes HMG1 and HMG2. PSA1 interaction in the GTP producing pathway is IMD3, identified uniquely at the first time point. IMD3 catalyzes the conversion of inosine monophospate in to xantosine-5-phoshate, which is further converted into GMP, GDP and GTP [32].

Another large group of proteins interacting with PSA1 is involved in cell wall morphology and cellular signaling. Several of these proteins contain sequences for potential phosphorylation and thus regulation by kinases and phosphatases. One heavily phosphorylated protein is HBT1, identified to interact with PSA1 at all time points. Plasma membrane casein kinase YCK1, found at time point two, has also been shown to participate in functions that regulate bud morphogenesis as well as vesicle trafficking [33–35]. APL5, Golgi-to-vacuole and possibly -plasma membrane transport protein, found uniquely at time point three, has been shown to suppress the deletion of YCK1 [36,37]. One possible YCK1-related protein associating with PSA1 uniquely at time point two is SAP155, an acidic protein with high asparagine content [38]. As YCK1 preferentially uses acidic proteins as substrate, the association with SAP155 could indicate some sort of regulation of SAP155 by YCK1. SAP155 itself is a positive regulator of SIT4 phosphatase that participates in cellular growth and cell cycle signaling including the nutrient response TOR-nutrient pathway [38]. The TOR pathway relays the information of nutrient status from cellular environment, ultimately regulating the cellular proliferation under changing environmental conditions [39]. The TOR system is also connected to the cell wall integrity pathway through small GTPase RHO1 [40]. The regulation of the RHO1 mediated responses is carried out by GTPase-activating proteins (GAPs) and nucleotide-exchange factors (GEFs) [41]. In our study we identified the RHO1 GEF factor TUS1 at time points two and four.

One intriguing facet of the PSA1 interactions is the one found with nuclear and mitochondrial proteins. It has been shown that several glycolytic enzymes participate in transcriptional regulation, apoptosis and other functions outside their normal glycolytic roles [42]. We identified nuclear proteins NUP145, MEC1, GAL4 and ORC2 as well as mitochondrial chaperone HSP60 and mitochondrial DNA polymerase subunit MIP1 interacting with PSA1. ORC2, identified at all time points is a subunit of the origin of recognition complex (ORC), which mediates the initiation of DNA replication under the control of the major cell cycle regulator CDC28 kinase [43]. MEC1 is a DNA integrity monitor [44], which initiates the signaling cascades leading to DNA repair and cell cycle arrest upon a genotoxic stress [45]. An interesting finding at time points 2–4 is the general galactose transcription factor GAL4, which is activated only in media containing galactose [46]. Our Verduin media was supplemented only with glucose so the galactose regulon should be in an inactive state. NUP145 is a subunit of the nuclear pore complex that cleaves itself *in vivo* to two functionally distinct polypeptides [47]. The PSA1 interactions with mitochondrial proteins were limited uniquely to the second-time point. HSP60 is the major mitochondrial matrix chaperone that enables the proper folding of the mitochondrion translocated proteins [48]. Other mitochondrial protein identified to interact with PSA1 is MIP1, a catalytic subunit of the mitochondrial DNA polymerase [49].

3.4. Conclusion

PSA1 participates in few larger pathways. Some of which are found at individual or few sequential time points, others scattered more randomly. The possible translocations of proteins, different regulatory, sensing and signaling events under varying conditions cannot be solved by examining only the interactome. A systematic approach by monitoring changes in subcellular locations, mRNA and protein quantities and phosphorylation state as well as enzymatic efficiencies and metabolite levels would provide a solid base for the elucidation of the role of individual interactions. Such exper-

iments generate large amounts of data and if these large datasets are to be publicly distributed and analyzed it becomes crucial that also the metadata, i.e., the data describing the experimental conditions as well as the analytical options need to searchable in computer-readable format.

Acknowledgments

The work was supported in part by Research Grants from Academy of Finland, by Research Grants from Technology Development Centre (TEKES), Sigrid Juselius Foundation and a grant from the Helsinki University Central Hospital Research Fund, Helsinki, Finland

Appendix A. Supplementary data

Supplementary data associated with this article can be found, in the online version, at doi:10.1016/j.ijms.2009.01.005.

References

[1] A.C. Gavin, P. Aloy, P. Grandi, R. Krause, M. Boesche, M. Marzioch, C. Rau, L.J. Jensen, S. Bastuck, B. Dumpelfeld, A. Edelmann, M.A. Heurtier, V. Hoffman, C. Hoefert, K. Klein, M. Hudak, A.M. Michon, M. Schelder, M. Schirle, M. Remor, T. Rudi, S. Hooper, A. Bauer, T. Bouwmeester, G. Casari, G. Drewes, G. Neubauer, J.M. Rick, B. Kuster, P. Bork, R.B. Russell, G. Superti-Furga, Nature 440 (2006) 631.
[2] A.C. Gavin, M. Bosche, R. Krause, P. Grandi, M. Marzioch, A. Bauer, J. Schultz, J.M. Rick, A.M. Michon, C.M. Cruciat, M. Remor, C. Hofert, M. Schelder, M. Brajenovic, H. Ruffner, A. Merino, K. Klein, M. Hudak, D. Dickson, T. Rudi, V. Gnau, A. Bauch, S. Bastuck, B. Huhse, C. Leutwein, M.A. Heurtier, R.R. Copley, A. Edelmann, E. Querfurth, V. Rybin, G. Drewes, M. Raida, T. Bouwmeester, P. Bork, B. Seraphin, B. Kuster, G. Neubauer, G. Superti-Furga, Nature 415 (2002) 141.
[3] N.J. Krogan, G. Cagney, H. Yu, G. Zhong, X. Guo, A. Ignatchenko, J. Li, S. Pu, N. Datta, A.P. Tikuisis, T. Punna, J.M. Peregrin-Alvarez, M. Shales, X. Zhang, M. Davey, M.D. Robinson, A. Paccanaro, J.E. Bray, A. Sheung, B. Beattie, D.P. Richards, V. Canadien, A. Lalev, F. Mena, P. Wong, A. Starostine, M.M. Canete, J. Vlasblom, S. Wu, C. Orsi, S.R. Collins, S. Chandran, R. Haw, J.J. Rilstone, K. Gandi, N.J. Thompson, G. Musso, P. St Onge, S. Ghanny, M.H. Lam, G. Butland, A.M. Altaf-Ul, S. Kanaya, A. Shilatifard, E. O'Shea, J.S. Weissman, C.J. Ingles, T.R. Hughes, J. Parkinson, M. Gerstein, S.J. Wodak, A. Emili, J.F. Greenblatt, Nature 440 (2006) 637.
[4] G. Rigaut, A. Shevchenko, B. Rutz, M. Wilm, M. Mann, B. Seraphin, Nature Biotechnology 17 (1999) 1030.
[5] J. Graumann, L.A. Dunipace, J.H. Seol, W.H. McDonald, J.R. Yates 3rd, B.J. Wold, DeshaiesF R.J, Molecular & Cellular Proteomics: MCP 3 (2004) 226.
[6] A.L. McCormack, D.M. Schieltz, B. Goode, S. Yang, G. Barnes, D. Drubin, J.R Yates 3rd., Analytical Chemistry 69 (1997) 767.
[7] H. Ge, A.J.M. Walhout, M. Vidal, Trends in Genetics 19 (2003) 551.
[8] J.K. Eng, A.L. McCormack, J.R. Yates, Journal of the American Society for Mass Spectrometry 5 (976) (1994) Äì 989.
[9] M. Mann, O.N. Jensen, Nature Biotechnology 21 (2003).
[10] V. Dancik, T.A. Addona, K.R. Clauser, J.E. Vath, P.A. Pevzner, Journal of Computational Biology 6 (1999) 327.
[11] K.G. Standing, Current Opinion in Structural Biology 13 (2003) 595.
[12] H. Hashimoto, A. Sakakibara, M. Yamasaki, K. Yoda, Journal of Biological Chemistry 272 (1997) 16308.
[13] R. Craig, R.C. Beavis, Bioinformatics, 20, Oxford, England, 2004, 1466.
[14] R. Craig, R.C. Beavis, Rapid Communications in Mass Spectrometry: RCM 17 (2003) 2310.
[15] J.A. Taylor, R.S. Johnson, Rapid Communications in Mass Spectrometry: RCM 11 (1997) 1067.
[16] M. Ashburner, C.A. Ball, J.A. Blake, D. Botstein, H. Butler, J.M. Cherry, A.P. Davis, K. Dolinski, S.S. Dwight, J.T. Eppig, M.A. Harris, D.P. Hill, L. Issel-Tarver, A. Kasarskis, S. Lewis, J.C. Matese, J.E. Richardson, M. Ringwald, G.M. Rubin, G. Sherlock, Nature Genetics 25 (2000) 25.
[17] M. Kanehisa, S. Goto, Nucleic Acids Research 28 (2000) 27.
[18] H. Hermjakob, L. Montecchi-Palazzi, C. Lewington, S. Mudali, S. Kerrien, S. Orchard, M. Vingron, B. Roechert, P. Roepstorff, A. Valencia, Nucleic Acids Research 32 (2004) D452.
[19] J.M. Cherry, C. Adler, C. Ball, S.A. Chervitz, S.S. Dwight, E.T. Hester, Y. Jia, G. Juvik, T. Roe, M. Schroeder, S. Weng, D. Botstein, Nucleic Acids Research 26 (1998) 73.
[20] U. de Lichtenberg, R. Wernersson, T.S. Jensen, H.B. Nielsen, A. Fausboll, P. Schmidt, F.B. Hansen, S. Knudsen, S. Brunak, Yeast (Chichester, England) 22 (2005) 1191.
[21] G.A. Dittmar, C.R. Wilkinson, P.T. Jedrzejewski, D. Finley, Science (New York, NY) 295 (2002) 2442.
[22] S.P. Bell, R. Kobayashi, B. Stillman, Science (New York, NY) 262 (1993) 1844.
[23] G. Micklem, A. Rowley, J. Harwood, K. Nasmyth, J.F. Diffley, Nature 366 (1993) 87.
[24] J.T. Pronk, H. Yde Steensma, J.P. Van Dijken, Yeast (Chichester, West Sussex) 12 (1996) 1607.
[25] G.F. Sprague Jr., Journal of Bacteriology 130 (1977) 232.
[26] D.J. Smith, A. Proudfoot, L. Friedli, L.S. Klig, G. Paravicini, M.A. Payton, Molecular and Cellular Biology 12 (1992) 2924.
[27] K. Duncan, R.M. Edwards, J.R. Coggins, The Biochemical Journal 246 (1987) 375.
[28] H. Cherest, Y. Surdin-Kerjan, Molecular & General Genetics: MGG 163 (1978) 153.
[29] T. Kodaki, S. Tsuji, N. Otani, D. Yamamoto, K.S. Rao, S. Watanabe, M. Tsukatsune, K. Makino, Nucleic Acids Research 3 (Supplement (2001)) (2003) 303.
[30] D. Thomas, Y. Surdin-Kerjan, Molecular & General Genetics: MGG 226 (1991) 224.
[31] M.E. Basson, M. Thorsness, J. Rine, Proceedings of the National Academy of Sciences of the United States of America 83 (1986) 5563.
[32] J.W. Hyle, R.J. Shaw, D. Reines, Journal of Biological Chemistry 278 (2003) 28470.
[33] L.C. Robinson, E.J. Hubbard, P.R. Graves, A.A. DePaoli-Roach, P.J. Roach, C. Kung, D.W. Haas, C.H. Hagedorn, M. Goebl, M.R. Culbertson, Proceedings of the National Academy of Sciences of the United States of America 89 (1992) 28.
[34] P.C. Wang, A. Vancura, T.G. Mitcheson, J. Kuret, Molecular Biology of the Cell 3 (1992) 275.
[35] X. Wang, M.F. Hoekstra, A.J. DeMaggio, N. Dhillon, A. Vancura, J. Kuret, G.C. Johnston, R.A. Singer, Molecular and Cellular Biology 16 (1996) 5375.
[36] C.R. Cowles, G. Odorizzi, G.S. Payne, S.D. Emr, Cell 91 (1997) 109.
[37] H.R. Panek, J.D. Stepp, H.M. Engle, K.M. Marks, P.K. Tan, S.K. Lemmon, L.C. Robinson, The EMBO Journal 16 (1997) 4194.
[38] M.M. Luke, F. Della Seta, C.J. Di Como, H. Sugimoto, R. Kobayashi, K.T. Arndt, Molecular and Cellular Biology 16 (1996) 2744.
[39] S. Wullschleger, R. Loewith, M.N. Hall, Cell 124 (2006) 471.
[40] M. Bickle, P.A. Delley, A. Schmidt, M.N. Hall, The EMBO Journal 17 (1998) 2235.
[41] T. Schmelzle, S.B. Helliwell, M.N. Hall, Molecular and Cellular Biology 22 (2002) 1329.
[42] J.W. Kim, C.V. Dang, Trends in Biochemical Sciences 30 (2005) 142.
[43] M. Weinreich, C. Liang, H.H. Chen, B. Stillman, Proceedings of the National Academy of Sciences 98 (2001) 11211.
[44] R. Kato, H. Ogawa, Nucleic Acids Research 22 (1994) 3104.
[45] K.A. Nyberg, R.J. Michelson, C.W. Putnam, T.A. Weinert, Annual Review of Genetics 36 (2002) 617.
[46] D. Lohr, P. Venkov, J. Zlatanova, The FASEB Journal: Official Publication of the Federation of American Societies for Experimental Biology 9 (1995) 777.
[47] M.T. Teixeira, S. Siniossoglou, S. Podtelejnikov, J.C. Benichou, M. Mann, B. Dujon, E. Hurt, E. Fabre, The EMBO Journal 16 (1997) 5086.
[48] M.Y. Cheng, F.U. Hartl, J. Martin, R.A. Pollock, F. Kalousek, W. Neupert, E.M. Hallberg, R.L. Hallberg, A.L. Horwich, Nature 337 (1989) 620.
[49] F. Foury, The Journal of Biological Chemistry (Print) 264 (1989) 20552.